Disruption of FADS2 gene in mice impairs male reproduction and causes dermal and intestinal ulceration

Chad K. Stroud,* Takayuki Y. Nara,* Manuel Roqueta-Rivera,† Emily C. Radlowski,* Peter Lawrence,†† Ying Zhang,†† Byung H. Cho,† Mariangela Segre,§ Rex A. Hess, J. Thomas Brenna,†† Wanda M. Haschek,§ and Manabu T. Nakamura[1],*,†**

Division of Nutritional Sciences,* Department of Food Science and Human Nutrition,† Department of Pathobiology,§ Department of Veterinary Biosciences,** University of Illinois at Urbana-Champaign, Urbana, IL 61801; Division of Nutritional Sciences,†† Cornell University, Ithaca, NY 14853

Abstract Delta-6 desaturase (D6D) catalyzes the first step in the synthesis of highly unsaturated fatty acids (HUFA) such as arachidonic (AA), docosapentaenoic (DPAn-6), and docosahexaenoic (DHA) acids, as well as the last desaturation of DPAn-6 and DHA. We created D6D-null mice (−/−), which enabled us to study HUFA deficiency without depleting their precursors. In −/−, no in vivo AA synthesis was detected after administration of [U-^{13}C]linoleic acid (LA), indicating absence of D6D isozyme. Unexpectedly, all of the −/− developed ulcerative dermatitis when fed a purified diet lacking D6D products but containing ample LA. The −/− also exhibited splenomegaly and ulceration in duodenum and ileocecal junction. Male −/− lacked normal spermatozoa with a severe impairment of spermiogenesis. Tissue HUFAs in −/− declined differentially: liver AA and DHA by 95%, and a smaller decrease in brain and testes. Dietary AA completely prevented dermatitis and intestinal ulcers in −/−. DPAn-6 was absent in −/− brain under AA supplementation, indicating absence of D6D isozyme for DPAn-6 synthesis from AA. This study demonstrated a distinct advantage of the D6D-null mice (−/−) to elucidate (1) AA function without complication of LA deprivation and (2) DHA function in the nervous system without AA depletion or DPAn-6 replacement seen in traditional models.—Stroud, C. K., T. Y. Nara, M. Roqueta-Rivera, E. C. Radlowski, P. Lawrence, Y. Zhang, B. H. Cho, M. Segre, R. A. Hess, J. T. Brenna, W. M. Haschek, and M. T. Nakamura. **Disruption of FADS2 gene in mice impairs male reproduction and causes dermal and intestinal ulceration. *J. Lipid Res.* 2009.** 50: **1870–1880.**

Supplementary key words arachidonic acid • delta-6 desaturase • docosahexaenoic acid • docosapentaenoic acid • eicosanoid • essential fatty acid • FADS3 • prostaglandin

Since the discovery of essential fatty acids by Burr and Burr (1), linoleic (LA) and α-linolenic acid (ALA) are identified as essential fatty acids that must be consumed in the diet. Once consumed, however, LA and ALA can both be desaturated and elongated into more highly unsaturated fatty acids (HUFA) such as arachidonic (AA), docosapentaenoic (DPA n-6), and docosahexaenoic (DHA) acids via the pathway shown in **Fig. 1A**. Delta-6 desaturase (D6D) performs the first and rate-limiting step in this process, as well as the last step of desaturation for DHA and DPA n-6 synthesis. The D6D gene FADS2 was cloned in 1999 (2), and subsequently, a human case of D6D deficiency was identified (3). The patient exhibited growth retardation accompanied by skin abnormalities, corneal ulceration, and feeding intolerance. Treatment with dietary AA and DHA restored normal growth and eliminated most other symptoms, underscoring the importance of the endogenous synthesis of these HUFAs.

AA is a precursor to a host of signaling molecules known as eicosanoids, which include thromboxanes, leukotrienes, prostacyclins, and prostaglandins produced from the oxygenation of AA by cyclooxygenase and lipoxygenase enzymes. However, the symptoms of classic essential fatty acid deficiency, growth retardation and dermatitis (1), are attributed to a loss of LA, not AA or eicosanoids. Because LA is an essential component of skin ceramides, LA deficiency results in the disruption of the skin's water barrier function (4) and heat loss from skin (5). These side effects make investigation of AA deficiency impossible by dietary manipulation without complications from LA deficiency.

DHA is found in large amounts in the retina, brain, and testes (6, 7). The role of DHA has been largely thought to be structural, increasing the fluidity of cellular mem-

This work was supported in part by the National Needs Fellowship Award AG 02-38420-11737 (C.K.S.) from the U.S. Department of Agriculture and Grant GM71534 from the National Institutes of Health (J.T.B.).

Manuscript received 30 January 2009 and in revised form 25 March 2009.

Published, JLR Papers in Press, April 7, 2009
DOI 10.1194/jlr.M900039-JLR200

Abbreviations: AA, arachidonic acid; ALA, alpha-linolenic acid; D5D, delta-5 desaturase; D6D, delta-6 desaturase; DHA, docosahexaenoic acid; DPA n-6, docosapentaenoic acid (n-6); HUFA, highly unsaturated fatty acid; LA, linoleic acid; PG, prostaglandin

[1]To whom correspondence should be addressed.
e-mail: mtnakamu@illinois.edu

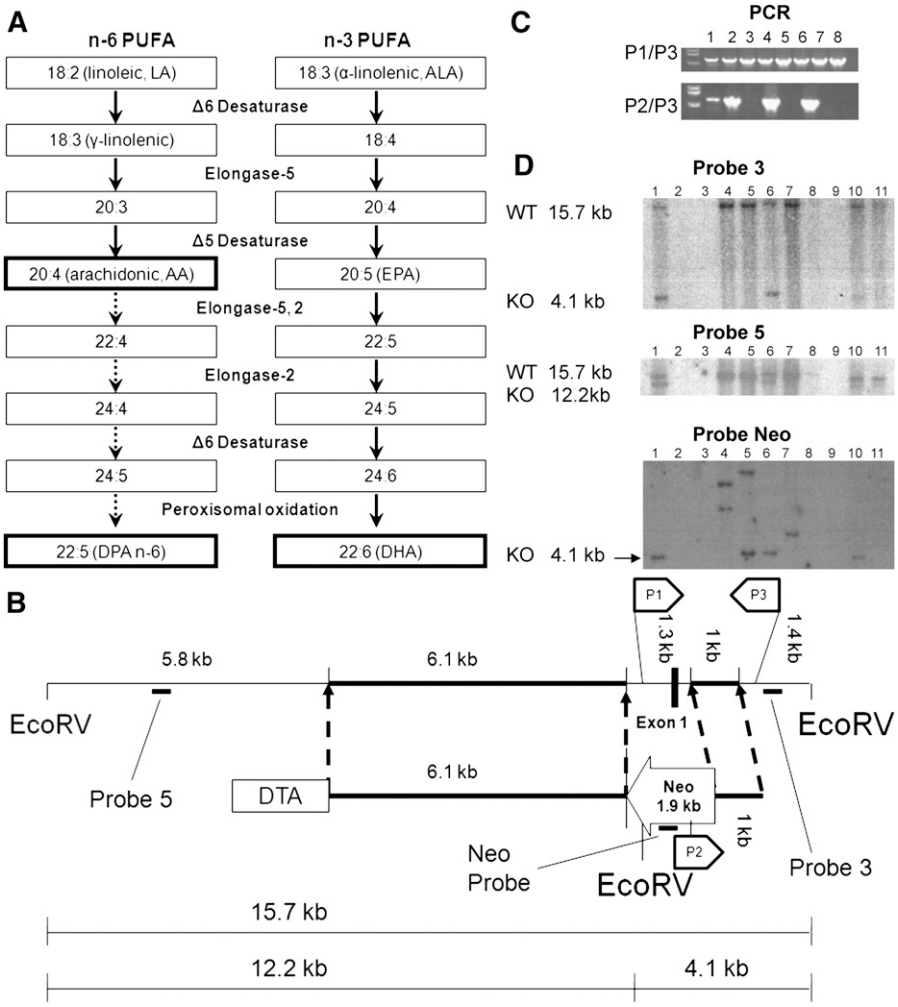

Fig. 1. Synthetic pathway of highly unsaturated fatty acids (HUFA) (A); design of the targeting vector (B); and selection of ES cells by PCR (C) and by Southern blot (D). A: In mammals, HUFA (AA, DPA n-6 and DHA) are synthesized from LA and ALA. B: The vector consists of neomycin resistant cassette (Neo), 6.1 kb and 1 kb flanking arms homologous to wild-type, and diphtheria toxin gene (DTA). Neo replaces a promoter and exon 1 region of *FADS2*. C: PCR screening of neomycin resistant ES cell lines. PCR with P1 and P3 primers (upper panel) shows presence of wild-type sequence in all cell lines, whereas PCR with P2 and P3 primers (lower panel) shows homologous recombination only in lanes 1, 2, 4 and 6. D: Southern blot analysis of EcoRV-digested DNA from PCR positive ES cells. Probe 3 (upper panel) shows a positive band of 4.1 kb on lanes 1, 6, and 10. Probe 5 (middle panel) also shows a positive band of 12.2 kb on lanes 1, 6, and 10. Neo Probe (bottom panel) shows positive bands of right size (4.1 kb) on lanes 1, 5, 6, and 10, whereas lanes 4, 5, and 7 show bands with different sizes indicating random incorporation of targeting vector.

branes, which is important for cell signaling (8). Recent work suggests DHA also plays a role as a precursor to docosanoids (9, 10) and as a modulator of growth factor signaling (11). However, a traditional model of DHA deficiency created by removal of all n-3 fatty acids from the diet is unable to unequivocally demonstrate the proposed functions in vivo. In the traditional model, DPA n-6 increases near stoichiometrically when DHA is decreased in brain, and likely, at least in part, compensates DHA function (12).

In humans, the testes also contain large amounts of DHA, which is a major fatty acid in the membranes of spermatozoa (13). Spermatozoa in rats contain large amounts of the DPA n-6, while mice have both DPA n-6 and DHA (7). DPA n-6 and DHA are found in the phospholipid membranes and are also precursors to very long chain HUFAs containing 26–32 carbons that are components of the sphingolipids present in spermatozoa (14). The exact function of these very long chain HUFAs in spermatogenesis is yet to be elucidated.

To overcome the obstacle for elucidating HUFA functions with a conventional model, we created a D6D −/− mouse. This model allows for the specific investigation of AA deficiency without the underlying complications due to LA deficiency. Also, this model would allow for investigation of DHA function in brain without a compensatory increase in DPA n-6 because D6D is also required for DPA synthesis from AA. Moreover, the D6D −/− model would enable investigation of DHA and DPA n-6 function in male reproduction without the underlying LA and AA deficiency.

EXPERIMENTAL PROCEDURES

Production of the D6D-null mouse

We created a targeting construct (Fig. 1B) to replace a total of 1.3 kb of the *FADS2* gene containing ~1 kb of the promoter, exon 1 and part of intron 1 with 1.9 kb of a neomycin-resistant cassette encoded to the opposite direction. Using a bacterial artificial chromosome (#AC026761) containing the entire *FADS2* genomic sequence of 129S6/SvEvTac mice, two homologous arms (6.1 kb and 1 kb in length) were synthesized using PCR and were incorporated into the pCS(+)NKP vector (provided by Dr. Victor Lin, Columbia University, NY). The diphtheria toxin gene (DTA) was inserted at the 5′ region to negatively select against a random incorporation of the target vector. The sequence of the construct was confirmed.

The clone was sent to the Transgenic Facility at Columbia University and electroporated into 129S6/SvEvTac embryonic stem (ES) cells. We received 192 neomycin resistant ES cell lines, which were then genotyped by PCR and Southern blot analysis. First, cells with homologous recombination were screened using PCR primer pairs for wild-type sequence and homologous recombination sequence of the FADS2 gene (Fig. 1C). Next, DNA from PCR positive ES cells were digested by EcoRV, separated by agarose gel electrophoresis, and hybridized with ^{32}P-lableld probes. Correct incorporation of the targeting sequence was confirmed using two different probes (Fig. 1D, Probe 3, Probe 5). Also, using a neomycin cassette specific probe, cells with random incorporation were identified and excluded (Fig. 1D, Probe Neo). Eleven cell lines that had a single copy of the vector at the targeting position were identified as suitable for injection into blastocysts of C57BL/6J to produce chimeric mice. Four chimeras (3 males and 1 female) were produced at Columbia University and then sent to University of Illinois. Two male chimeras, bred with +/+ C57BL/6J females, produced pups with agouti coats signifying germ line transmission. Of these, one litter produced pups testing positive, via PCR, for the transmission of the *FADS2* mutant gene, resulting in a heterozygous male and female. These two founders (F1) were used to start the breeding colony used for subsequent studies.

Animal studies

Heterozygous males and females were used for all of the breeding to produce three genotypes reported in this study. All experimental animals were nursed by +/− mothers fed standard laboratory diet. Pups were genotyped using DNA extracted from 5 mm tail snips via PCR. Four primer sets, flanking exon 1 were used to amplify both knockout and wild-type regions. All animal work was approved by the University of Illinois Institutional Animal Care and Use Committee. Studies characterizing male and female mice were repeated twice.

D6D activity and expression

Five-week old F2 −/− and +/+ females (n = 3 each) were fed a fat-free diet for one week to induce desaturases. Animals were euthanized by cervical dislocation, and the brain, heart, stomach, and liver were removed. A fraction of liver was flash frozen for RNA analysis and a fraction reserved for assaying desaturase activity. Remaining tissues were flash frozen for RNA analysis. Desaturase activity was measured with slight modifications of a method described previously (15). Briefly, freshly removed liver was homogenized, and a microsome fraction was separated by differential centrifugation. The microsomes were incubated for 15 min at 37°C in the medium containing ^{14}C-LA, ATP, and NADH. After methylating using 3M methanolic HCl, LA and the desaturation product (18:3) were separated via thin layer chromatography on a silica gel G plate (Analtech, Newark, DE) impregnated with $AgNO_3$, and the radioactivity was measured.

D6D gene expression was measured by real-time PCR using SYBR Green fluorescent dye as previously described (16). Briefly, liver was homogenized in TRIzol reagent (Invitrogen, Carlsbad, CA) and total RNA extracted. MultiScribe Reverse Transcriptase (Applied Biosystems, Foster City, CA) along with random hexamers, was used to synthesize cDNA. Real-time quantitative PCR with SYBR Green fluorescent dye (Applied Biosystems) was used to analyze RNA which was quantified relative to 18S rRNA.

In vivo D6D activity analysis

Eight-week-old (F3) +/+ and −/− (two males and two females for each genotype) were given 5 mg of [U-^{13}C]LA (Sigma-Aldrich, St. Louis, MO), mixed with 0.1 ml olive oil, by oral gavage. Gas chromatography-combustion-isotope ratio mass spectrometry was used to analyze ^{13}C-fatty acids (17). After 48 h, mice were euthanized by CO_2 inhalation. Liver, brain, heart, stomach, testes, and remaining carcass were flash-frozen for lipid analysis. Total lipids were extracted and converted to fatty acid methyl ester, as described under fatty acid analysis. The mean δ^{13}C for liver AA in the −/− mice was found to reflect a stable baseline in the natural abundance range (−21.4 ± 1.8‰, mean ±SD) and was very similar to the values found for whole carcass 16:0 and 18:0 (−21.8 ± 1.2‰ and −20.8 ± 1.6‰, respectively), two fatty acids that showed no differences between dosed +/+ and −/− mice. This baseline value was subtracted from each of the δ^{13}C for the individual fatty acid methyl ester to yield delta-over-baseline.

Female characterization

At weaning (21 days old), −/−, +/−, and +/+ females (n = 3 for each group; F2) were fed AIN93G diet (18) (Research Diets, New Brunswick, NJ) ad libitum. AIN93G is a purified diet that contains soybean oil at 7% of diet as the sole source of dietary fat with sufficient LA (3.8% of diet) and ALA (0.6% of diet) but no D6D products. Animals were group housed by genotype and weighed every other day and gross observations, both physical and behavioral, were made routinely. Animals were euthanized at 21 weeks of age by CO_2 inhalation. At necropsy, selected organs were weighed, tissue samples were collected, and flash-frozen for fatty acid analysis or fixed in 10% neutral buffered formalin for histological evaluation. Tissues (skin, liver, brain, eye, heart, kidney, adrenal, thymus, spleen, stomach, small and large intestine, lymph nodes, uterus, vagina and ovaries, mammary gland, salivary gland, pancreas, skeletal muscle, and urinary bladder) were embedded in paraffin, sectioned at 4 μm, stained with hematoxylin and eosin, and examined by light microscopy. Eyes were fixed in Davidson's fixative (19) and transferred to 10% neutral buffered formalin after 24 h. The gastrointestinal tract was prepared in a "Swiss-roll"style before fixation to enable examination of the whole gastrointestinal tract.

Male characterization

Similarly to the females, 21-day-old F3 males (seven −/−, five +/−, and four +/+) were fed AIN93G diet ad libitum. Mice were singly housed, and gross observations were made routinely. The animals were weighed every other day, and food intake was recorded weekly. Beginning at 5–6 weeks of age, −/− males were housed with +/+ 129S6/SvEvTac females for 4 days out of every 14 to determine fertility. This continued until animals were euthanized at 15 or 19 weeks old (before and after the onset of dermatitis). In addition, +/+ males were each housed with +/+ 129S6/SvEvTac females once to ensure fertility. Euthanasia and necropsy was performed as described for females except that testis and epididymis were examined. Testes were fixed as described for eyes above.

AA supplementation

21-day-old +/+ and −/− females (n = 3; F3) were fed ad libitum AIN93G diet supplemented with a 0.4% (w/w) AA (ARASCO, Martek Biosciences, Columbia, MD). Animals were euthanized at 8 months of age by CO_2 inhalation. Skin samples were obtained for PGD_2 measurement and for histological evaluation. Skin and brain samples were also collected for fatty acid analysis.

Positional analysis of double bonds in fatty acids

Total lipids were extracted from each tissue and fatty acid methyl esters were synthesized as described in the fatty acid analysis. Double bond locations were determined as previously reported (20). Briefly, 1-methyleneimino-1-ethenylium (CH_2=C = N^+=CH_2), a product of chemical ionization of acetonitrile adds to fatty acid double bonds to yield an adduct which dissociates into unique fragments upon collisional activation, enabling determination of double bond position.

Fatty acid analysis

Tissue fatty acids were analyzed as previously reported with slight modifications (21, 22). Briefly, tissues were homogenized in methanol and lipids extracted with chloroform (2:1, v/v) containing 0.1% β-hydroxytoluene to prevent oxidation. C17:0 phosphatidylcholine, cholesterol esters and triacylglycerol were added as internal standards. Liver lipids were fractionated via thin layer chromatography. Lipids were not fractionated for other tissues. Three M methanolic HCl (Supelco, Bellefonte, PA) was used to methylate fatty acids (90 min at 75°C). Fatty acid species were identified by HP5890 gas chromatography (Agilent Technologies, Wilmington, DE) using a 30 m × 0.25 mm Omegawax capillary column (Supelco).

Skin PGD_2 assay

Prostaglandin extraction from skin was based on the method by Sugimoto et al. (23). Skin portion from the back of the mouse was removed (intrascapular region), weighed, and minced on ice. Tissue was then homogenized in ice-cold phosphate buffered saline containing 10 μM indomethacin. An equal volume of acetone was added to the sample, mixed, and incubated on ice for 5 min. Precipitate was removed by centrifugation at 2000 *g* for 10 min at 4°C. Supernatants containing prostaglandin were blown down with nitrogen and resuspended in enzyme immunoassay buffer. Methoximation of samples was performed and PGD_2 was measured using the PGD_2-Mox EIA kit (Cayman Chemical, Ann Arbor, MI).

Statistical analysis

Data were analyzed using Statview 5.0.1 (SAS Institute, Cary, NC). All data are reported as mean ± SD. Data of three genotypes were compared by one-way ANOVA followed by Tukey's posthoc test. Student's *t*-test was used to analyze data between two genotypes. Statistical significance was set at $P < 0.05$.

RESULTS

Delta-5 desaturation of LA occurs when expression of D6D is halted

Before characterizing the phenotype of this newly created −/− mouse model, we sought to verify the lack of D6D in −/− mice. As expected, *FADS2* transcription was halted as seen in **Fig. 2A**. Next we measured activity by incubating liver microsomes with ^{14}C-LA and quantifying resulting ^{14}C-labeled desaturation products. Fig. 2A shows that the −/− microsomes added the third double bond to ^{14}C- LA at approximately 20% of the microsomes from the +/+ although this activity assay did not allow us to determine the position of the double bond added.

Gas chromatography for liver phospholipids showed unknown peaks present only in the −/−, in particular a peak with a significant size near 20:3 n-6 (Fig. 2B). Covalent adduct chemical ionization (Fig. 2C) identified the peak near 20:3 n-6 as 20:3 (Δ 7, 11, 14), a fatty acid produced from LA through desaturation by delta-5 desaturase (D5D) followed by elongation (Fig. 2D). Elongation products of ALA, namely 20:4 (Δ 7, 11, 14, 17) and 22:4 (Δ 9, 13, 16, 19), were also identified by covalent chemical ionization in a small quantity in −/− (data not shown), indicating that ALA was also desaturated by D5D and then elongated in the −/− animals in the same manner as LA (Fig. 2D). No significant change in D5D mRNA was observed in liver of D6D-null mice (data not shown), showing that the accumulation of 20:3 (Δ 7, 11, 14) in −/− was not dependent on upregulation of D5D. Thus, the accumulation of 20:3 (Δ 7, 11, 14) is likely due to loss of competition from D6D at the step of linoleic acid desaturation, as well as loss of competition at the step of incorporation of fatty acids into phospholipids.

No AA synthesis from LA is detected in vivo in the D6D −/− mouse

Among putative fatty acid desaturase genes in the mouse genome, we identified three genes homologous to FADS2, namely FADS3, FADS6, and 4833423E24Rik. Transcripts of all three genes were found in liver, and FADS3 mRNA was nearly three times higher in the −/− (Fig. 2E). A predicted amino acid sequence of the FADS3 gene has the highest homology to FADS2 (63% identical) among any known fatty acid desaturases, suggesting that FADS3 may be involved in the synthesis of HUFAs.

Because of the presence of putative desaturase transcripts, we determined if any HUFA synthesis was still present in the −/− animals. Forty-eight h after oral gavage with 5 mg [U-^{13}C]LA, liver total fatty acids from −/− mice failed to show any presence of ^{13}C labeled D6D products, 18:3 n-6, 20:3 n-6 or AA (20:4 n-6) (Fig. 2F). However the same figure shows the presence of the elongated ^{13}C labeled 20:2 n-6 (synthesized via elongase) and also shows the presence of ^{13}C labeled 20:3 (Δ 7, 11, 14) (synthesized by D5D and elongase enzymes). The presence of ^{13}C labeled 20:3 (Δ 7, 11, 14) in the +/+ showed that delta-5 desaturation of LA was not unique to −/− but occurred in the +/+ as well (Fig. 2F), although +/+ did not accumulate 20:3 (Δ 7, 11, 14) in liver phospholipids as −/− did (Fig. 2B). This in vivo activity analysis demonstrated absence of D6D isozyme capable of delta-6 desaturation of LA in the mouse liver. Also, lack of labeling in AA in the −/− demonstrated that there is no alternative pathway of AA synthesis either in liver through Δ8 desaturation of 20:2 n-6 when the FADS2 gene is knocked out. Consistent with this absence of AA synthesis in liver of the D6D-null mice, protein encoded by the FADS3 gene showed neither

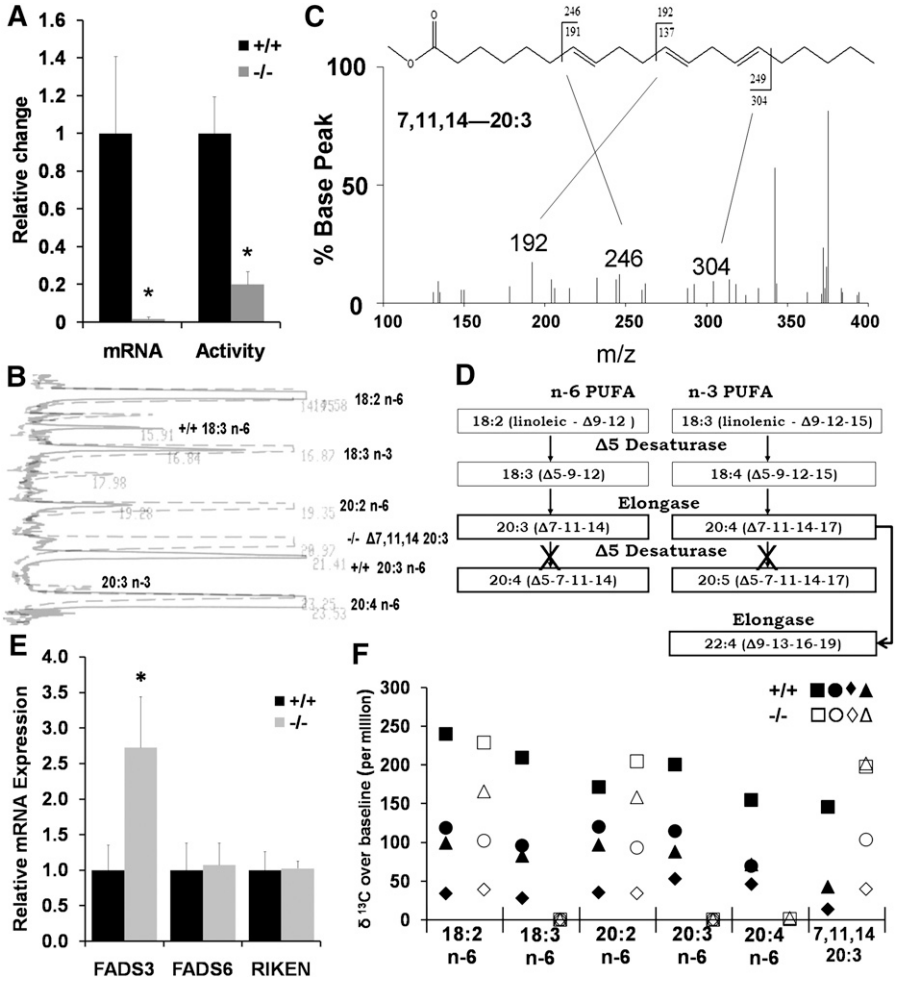

Fig. 2. Determination of absence of D6D isozyme. A: Gene expression measured by SYBR Green demonstrates halted transcription of *FADS2*, whereas activity of desaturating ^{14}C-LA was present in liver microsomes of the knockout. The double bond position could not be determined by this activity assay. Values are the mean ± SD (n = 3); * $P < 0.05$; Student's *t*-test. B: Separation of liver phospholipid fatty acids by gas chromatography. 18:3 n-6 and 20:3 n-6 peaks were absent in the −/− (dashed). A peak that was unique to −/− near 20:3 n-6 was identified as Δ7,11,14 20:3. C: Output of covalent adduct chemical ionization GC/MS that identified the presence of 7,11,14-20:3 in liver phospholipids. D: Summary of desaturation, elongation pathway for the fatty acids detected in the liver from −/−. E: Transcripts of putative fatty acid desaturases in liver: FADS3, fatty acid desaturase 3; FADS6, fatty acid desaturase 6; RIKEN, 4833423E24Rik. Values are the mean ± SD (n = 3); * $P < 0.05$ by Student's *t*-test. F: In vivo ^{13}C labeling of liver fatty acids 48 h after administration of [U-^{13}C]LA. Values of individual animals (n = 4 each) are shown. D6D desaturation products 18:3 n-6, 20:3 n-6, and 20:4 n-6 were absent in all −/− animals.

Δ6- nor Δ8-desaturase activity when tested by transfecting an FADS3 expression vector to HepG2 and HEK293 cells (unpublished data).

Female −/− exhibit a variety of pathology including dermatitis, enlarged spleen and liver, and intestinal ulcer

To characterize phenotype of the −/− mouse, female +/+, +/−, and −/− animals were fed AIN93G diet, a nutritionally adequate, purified diet that contains sufficient LA and ALA, but no D6D products from weaning. The −/− females showed no significant differences in growth compared with the +/− and +/+ (**Fig. 3A**). At approximately 120 days of age, all of the −/− animals developed slight skin irritation which resulted in obsessive scratching behavior that ultimately resulted in severe ulcerative dermatitis around the face, neck, and ears in all −/− mice. After skin lesions appeared, weight loss was identified at approximately 135 days of age at which time the mice were euthanized. At necropsy, −/− mice had severely reduced thymus, enlarged spleen (4.0×), liver (1.6×) and kidney (1.3×) (Fig. 3B). Also, −/− animals had multiple gastric trichobezoars (hair balls formed from licking ulcerated skin treated with ointment), which were presumably responsible for the reduction in food intake and weight loss observed toward the end of the study.

Histologically, the dermatitis was characterized by ulcers with inflammation extending through the dermis and underlying muscle (**Fig. 4G**, 4H). Small scattered ulcers were also present within the intestinal tract, primarily at the ileocecal junction and sometimes in the duodenum and

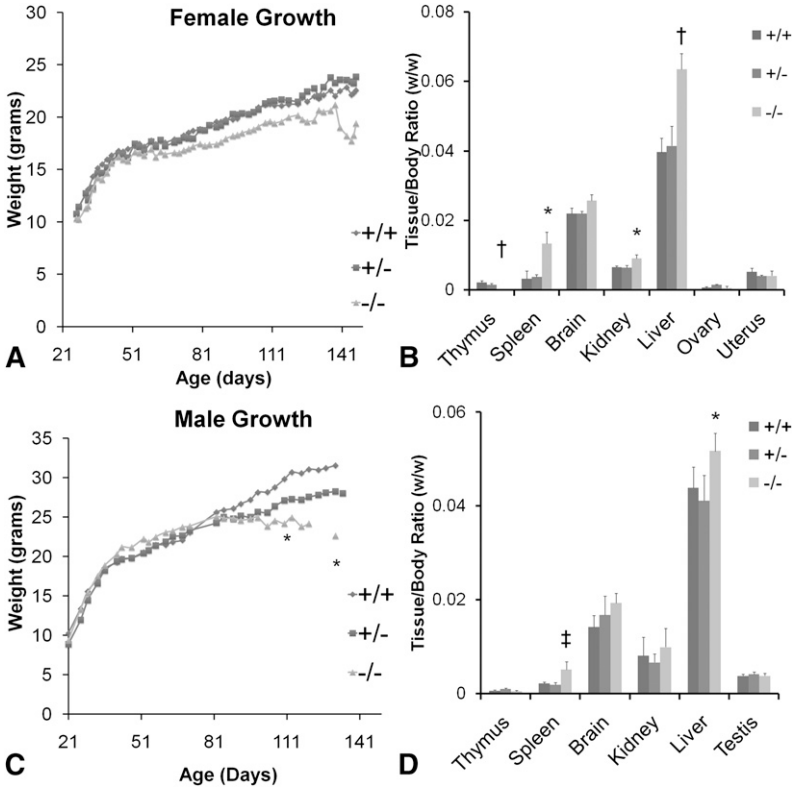

Fig. 3. Growth and relative organ weights of +/+, +/− and −/− animals fed AIN93 diet after weaning. A: Growth in the females showed no significant differences. B: Organ weight of females at ∼21 weeks of age. C: Growth in the males. Weight of −/− plateaued after 80 days of age. D: Organ weight of males at ∼20 weeks of age. *$P < 0.05$; †$P < 0.01$; ‡$P < 0.001$ by Student's *t*-test (−/− compared with +/+); n = 3–6.

ileum (figure not shown). Lymphoid depletion was prominent in the cortex of the thymus (Fig. 4C versus 4D), and in the white pulp of the spleen of the −/− (Fig. 4E versus 4F). The red pulp was expanded due to variable erythroid and myeloid hyperplasia (Fig. 4F). The ovaries of the −/− had fewer follicles, impairment of follicle maturation, and luteinization of stromal cells (Fig. 4A versus 4B). Ovaries of the −/− weighed less than the +/+, but did not reach statistical significance (10 ± 7 mg vs. 16 ± 9 mg, n = 6 each), whereas uterus of the −/− was significantly lower than the +/+ (79 ± 35 mg versus 123 ± 33 mg, n = 6 each, $P < 0.05$). However, weight of ovaries and uterus of −/− was not significantly different from +/+ when expressed relative to body weight (Fig. 3B).

Male −/− exhibit a similar phenotype to female −/−, impaired sperminogenesis and infertility

Male −/− animals were characterized using the same feeding protocol as the females. Initially, male −/− exhibited nearly identical growth patterns compared with +/− and +/+. However, at approximately 80 days of age, growth plateaued in the −/−, and the difference became significant at 110 days of age between the +/+ and −/− (Fig. 3C). As in the female −/−, all of the male −/− developed skin irritation leading to ulcerative dermatitis at approximately 120 days of age. Similarly to females, male −/− also had enlarged spleens (2.6×) and livers (1.2×) although the changes were not as severe as in females (Fig. 3D). Unlike females, thymus atrophy was not present in the male −/− (Fig. 3D). Testes of the $^{-/-}$ weighed slightly but significantly less than the +/+ (92 ± 11 mg, n = 9 vs. 106 ± 9 mg, n = 6, $P < 0.05$). However, the difference disappeared when expressed relative to body weight (Fig. 3D). Histological changes were similar to females with ulcerative dermatitis (**Fig. 5A**, 5B), ulcers at the ileocecal junction (Fig. 5G) and occasionally in the duodenum (Fig. 5H); some with inflammation extending transmurally with resulting localized peritonitis.

Fertility was also evaluated. Male −/− were singly housed with a +/+ female for 4 days out of every 14 days beginning at 5–6 weeks of age until termination; different female mice were used at each time point. All mice engaged in copulatory behavior, verified by visual observation. None of the −/− males produced viable litters, although 40 total matings were performed. All four of the +/+ produced one viable litter to verify fertility of male +/+ and female breeders. In contrast, the −/− males were able to impregnate females when supplemented with HUFAs (data not shown), demonstrating the essentiality of HUFAs in male fertility.

Histologically, spermatogenesis was severely impacted (Fig. 5C–5F). Normal spermatozoa or elongated spermatids were absent in the seminiferous tubules of the −/− males (Fig. 5D). The lesion in the testes very clearly demonstrates impaired spermatid elongation. In the −/− testes, spermatogonia, spermatocytes, and round spermatids appeared to have normal morphology, while elongated spermatids and spermatozoa were lacking (Fig. 5D). The lumen of −/− epididymides lacked mature spermatozoa but contained sloughed spermatids and spermatocytes (Fig. 5F).

HUFAs in tissues from −/− decline differentially

Fig. 6 shows that all tissues examined had decreased levels of AA and DHA in the −/− animals in varying degrees. Liver phospholipids showed a ∼2× increase of LA in both

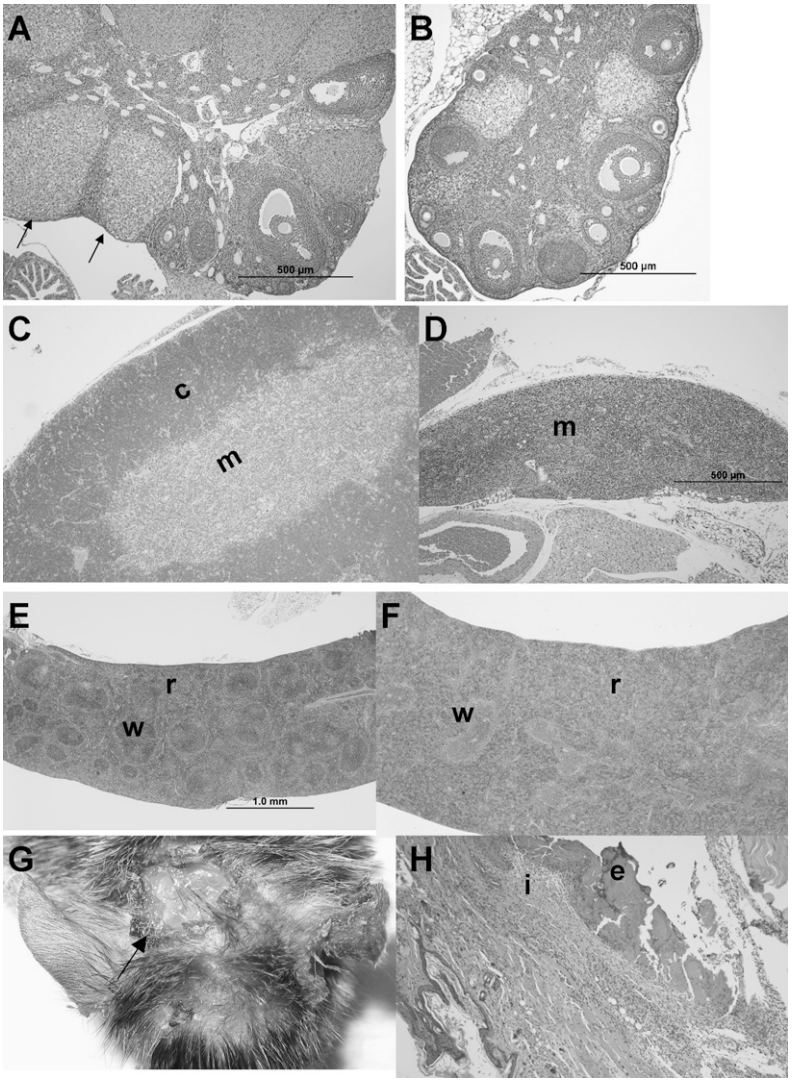

Fig. 4. Histology of female mice fed AIN93 diet from weaning. +/+, +/−, and −/− animals were euthanized at the manifestation of dermatitis in −/− (∼21weeks of age). No difference in histology was observed between +/+ and +/−. A: Ovary from +/+ mouse shows normal follicle maturation with multiple corpora lutea (arrows), whereas (B) ovary from −/− mouse is smaller and lacks mature corpora lutea. C: Thymus from +/+ mouse has normal cortex (c) and medulla (m), while (D) thymus from −/− mouse is small with severe cortical lymphocyte depletion. E: Spleen from +/+ mouse has normal white (w) and red (r) pulp. F: Spleen from −/− mouse is greatly enlarged (4.0×) due to expanded red pulp (r) whereas white pulp (w) is depleted. G: Ulcerative dermatitis (arrow) on head of −/− at necropsy. H: Ulceration of −/− skin with superficial exudation (e) and severe inflammation (i) of the dermis. H and E stain.

male and female −/− with a sharp reduction (approximately 95%) of both AA and DHA. In addition, a previously unseen fatty acid (20:3 Δ 7, 11, 14) composed ∼10% of phospholipid fatty acids (Fig. 6A, 6C). Whereas fatty acid composition in liver phospholipids and other tissues were similar between +/+ and +/− (Fig. 6), fatty acids in cholesterol ester from liver of the +/− tended to fall in between those of the +/+ and −/− (**Fig. 7A**), indicating that a single copy of D6D gene cannot fully compensate for HUFA synthesis. A mild increase of triglycerides (∼2×) was observed in liver from the −/− (Fig. 6G). This increased triglycerides partially contributed to the increased liver weight in the −/− animals (Fig. 3B, 3D). Fatty acids in the heart (Fig. 7B) closely resembled those in liver phospholipids, with AA and DHA decreasing by 75% and 73%, respectively.

In the brain, similarly to liver phospholipids, LA increased ∼2×, while 20:3 (Δ 7, 11, 14) increased to ∼5% of total fatty acids in both male and female −/− (Fig. 6B, 6D). Unique to the brain, however, is the more mild decrease of AA and DHA, suggesting a stronger conservation of HUFAs in the brain compared with other tissues. In the female brain, AA decreased by 40%, while DHA decreased only by 15% (Fig. 6B). Male brains contained 45% lower AA and 33% lower DHA (Fig. 6D).

In the mouse, spermatozoa contain a significant amount of DPA n-6, not widely seen in other tissues. The testes and cauda epididymis both showed marked reductions in HUFAs, but no other significant fatty acid changes (Fig. 6E, 6F). In the −/− testes, AA decreased by 91%, DHA decreased by 54% and DPA n-6 decreased by 93% (Fig. 6E). Similarly, in the cauda epididymis, AA decreased by 72% and DPA by 77%. DHA decreased by 42% although the decrease in DHA did not reach statistical significance (Fig. 6F). In both the testes and epididymis, the amount of 20:3 (Δ 7, 11, 14) increased substantially, to 7.5% and 1.5% of total fatty acids, respectively (Fig. 6E, 6F).

AA supplementation prevents dermatitis and intestinal ulcer, and restores brain AA without accumulation of DPA n-6

AA supplementation at 0.4% of diet completely prevented the onset of the ulcerative dermatitis and intestinal ulcer in the −/− when examined at 8 months of age. When fed an AA deficient diet (AIN93G), AA in the skin decreased by 75% at 4 months of age (**Fig. 8A**). However,

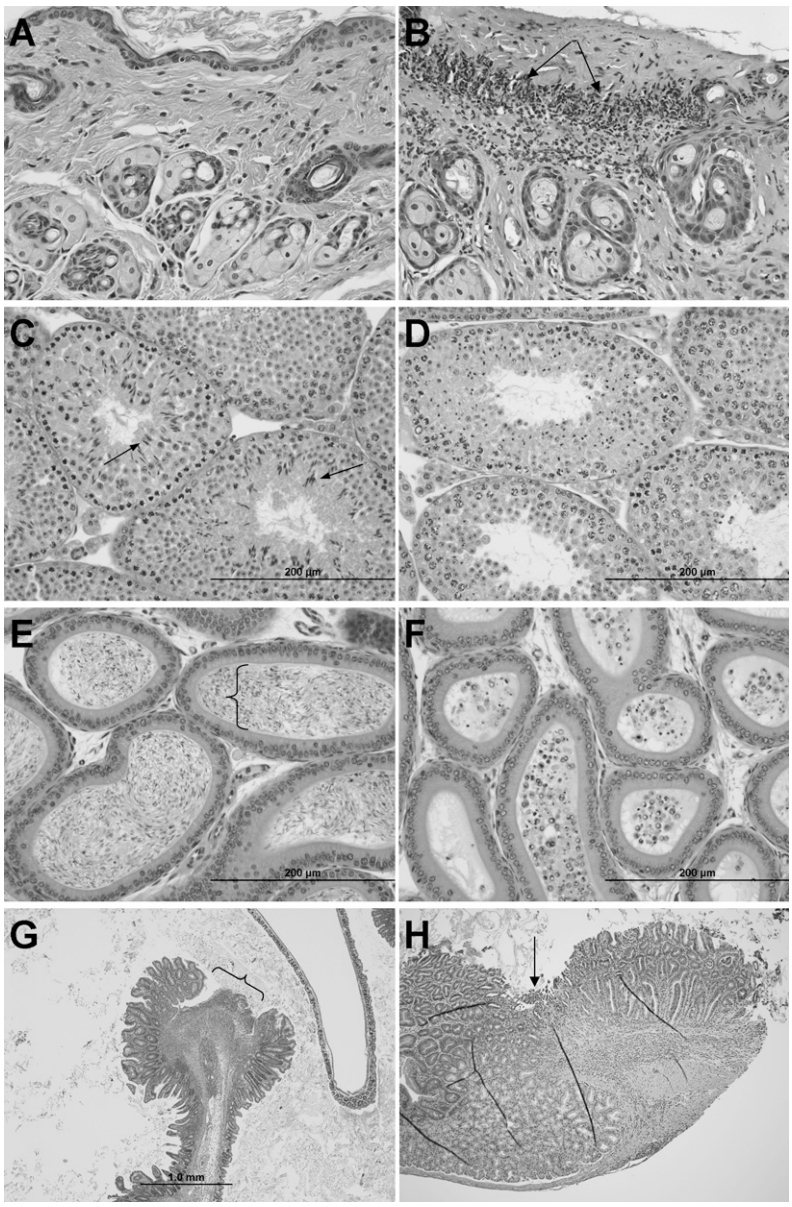

Fig. 5. Histology of male mice fed AIN93 diet from weaning. +/+, +/−, and −/− animals were euthanized at the manifestation of dermatitis in −/− (∼20 weeks of age). No difference in histology was observed between +/+ and +/−. Skin from a −/− mouse, (A) unaffected area, and (B) with ulcerative dermatitis (arrows). C: Seminiferous tubules in testis from +/+ mouse shows all stages of spermatogenesis including elongated spermatids (arrows) and spermatozoa (in lumen), while (D) testis from −/− mouse shows lack of elongated spermatids and spermatozoa. E: Epididymis from +/+ mouse contains viable spermatozoa (bracket), while (F) epididymis from −/− mouse contains sloughed round spermatids (smaller cells with round nuclei) and spermatocytes (larger cells with more dispersed chromatin). G: The intestine from a −/− mouse has an ulcer (bracket) at the ileocecal junction. H: Duodenum ulcer (arrow) in −/− with inflammation extending into the submucosa. No intestinal ulceration was found in +/+ and +/− animals. H and E stain.

skin AA is restored in the AA-supplemented −/− (Fig. 8A). Fig. 8B shows a similar decrease in PGD_2 in the skin from −/− fed the AIN93 diet. Interestingly, supplementation of AA did not completely restore skin PGD_2 synthesis (∼50%), although AA levels were higher in the −/− (Fig. 8A, 8B). After AA supplementation, brain fatty acids showed normal levels of AA with a 35% decrease in DHA (Fig. 8C). Of particular importance is that DPA n-6, which increases in a traditional n-3 deficient model (12), did not appear in the −/− even though DHA was decreased in brain (Fig. 8C). Thus, the data indicate that the last step of desaturation of DPA n-6 and DHA is also disabled in this −/− model.

DISCUSSION

Our first goal was to determine if there is any D6D isozyme that can desaturate the first step as well as the last step of DHA and DPA n-6 synthesis. All of our data support the absence of an isozyme. First, there is no in vivo conversion of [U-^{13}C]LA to D6D products in liver of −/−, demonstrating absence of D6D isozyme. We recently reported that a single enzyme encoded by the FADS2 gene possesses both Δ6 and Δ8 desaturase activities (24). This dual enzyme activity is consistent with the results of the current study that demonstrated absence of Δ8 desaturation pathway of AA synthesis when the FADS2 gene is knocked out. Second, analysis of tissue fatty acids of −/− animals showed marked decline of D6D products and presence of D5D desaturation products of both LA and ALA, suggesting absence of n-3 specific D6D either. The rate of decrease in brain DHA (by 33% in male) is similar to the rate achieved by a traditional DHA deficiency model using dietary deprivation of n-3 fatty acids, for example, a decline by 37% in male rats of compatible age (12). Furthermore, when −/− were supplemented with AA but deprived of dietary n-3 fatty acids for 7 months, brain fatty acids failed to show any DPA n-6 increase, indicating that no D6D

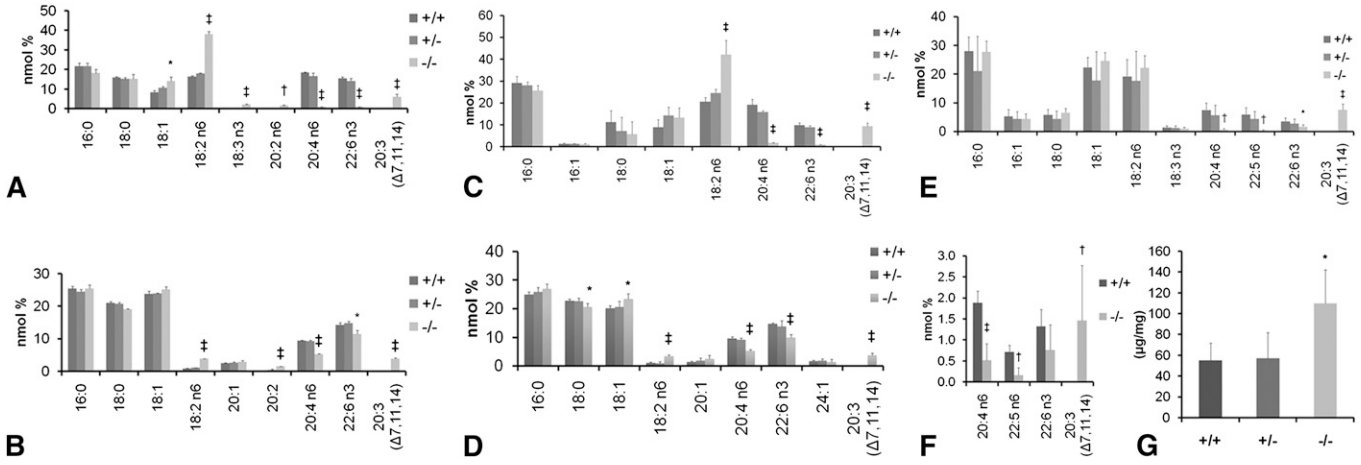

Fig. 6. Tissue fatty acid profile and liver triglycerides from ++, +/−, and −/− fed AIN93 diet from weaning. Tissues were analyzed at the onset of dermatitis in the −/− animals. A: Fatty acids in liver phospholipids from females and (C) from males. B: Fatty acids in brain total lipid extracts from females and (D) from males. E: Fatty acids in testis total lipid extracts. F: Fatty acids in cauda epididymis total lipid extracts. G: Liver triglycerides in males. $^{*}P < 0.05$; $^{\dagger}P < 0.01$, $^{\ddagger}P < 0.001$by Student's *t*-test (−/−compared with +/+); n = 3 (females), 4 (males).

isozyme exists for the last step of desaturation for DHA and DPA n-6 synthesis in the mouse. Thus, as expected, this −/− mouse can be used as a new animal model for elucidating 1) AA function without complications of LA deficiency and 2) the function of DHA in the brain, without compensatory accumulation of DPA n-6.

One unanticipated result was the appearance of skin lesions which manifested at approximately 17 weeks of age in the −/− on a diet with ample amounts of LA. Because AA supplementation completely prevented the dermatitis in the −/−, our study demonstrated that in addition to LA, AA is also required to maintain normal function of skin in mice. Our results are consistent with the human case of D6D deficiency in *1*) manifestation of dermatitis even while adequately consuming LA and *2*) subsequent disappearance of most symptoms including dermatitis by HUFA supplementation (3). It should be noted however skin and hair abnormalities remained after HUFA treatment in the human case, whereas our −/− did not exhibit skin or hair abnormalities after AA supplementation. This difference can be explained by differential expression of desaturases in sebaceous glands between mice and humans. Humans express D6D to produce 16:1 n-10 in the sebaceous gland for skin lipid synthesis whereas mice express stearoyl CoA desaturase-1 to synthesize 16:1 n-7 in the same gland (25). Consistent with this explanation, stearoyl CoA desaturase-1 knockout mice exhibited skin abnormality that could not be rescued by dietary oleic acid (26).

The exact mechanism by which AA can prevent ulcerative dermatitis in the −/− is yet to be determined. However, an inbred mouse strain, NC/Nga spontaneously begins scratching around the head, ears and nose region, and develops ulcerative dermatitis beginning at 8 weeks of age (27), a similar phenotype to our −/− mice. When applied topically, PGD_2 was the most potent prostanoid in preventing the scratching behavior and subsequent development of dermatitis in this strain (28). A gradual decrease in prostaglandin D synthase expression is the likely cause of the dermatitis in the NC/Nga strain (23). The −/− mouse also showed diminished PGD_2 when skin AA decreased, suggesting decreased availability of AA for PGD_2 synthesis as a possible mechanism of dermatitis development in our model.

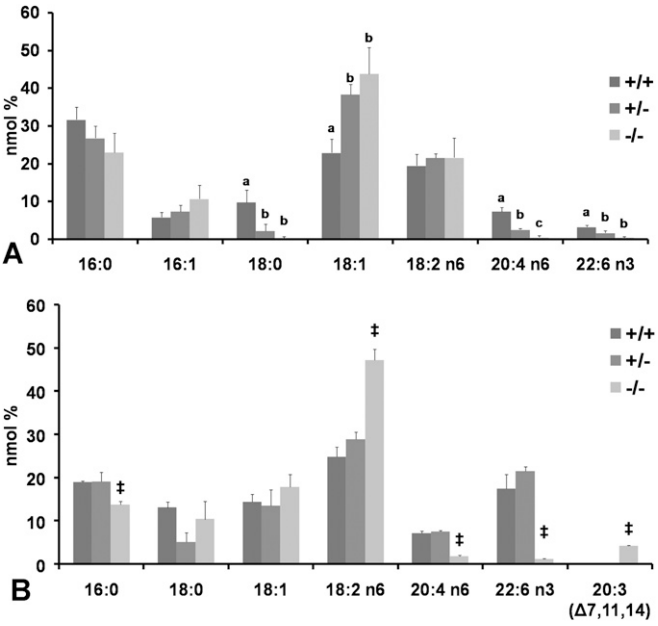

Fig. 7. Tissue fatty acid profile. A: Female liver cholesterol esters from D6D +/+, +/− and −/−. Fatty acids from +/− fall in between those of +/+ and −/−, indicating that a single copy of the D6D gene is unable to fully support HUFA synthesis. Difference between data with different letters are significant by Tukey's test after ANOVA ($P < 0.05$). B: Male heart fatty acids from D6D +/+, +/− and −/−. Moderate amounts of 20:3 (7, 11, 14) were accumulated. Student's *t*-test (between +/+ and −/−); $^{\ddagger}P < 0.05$.

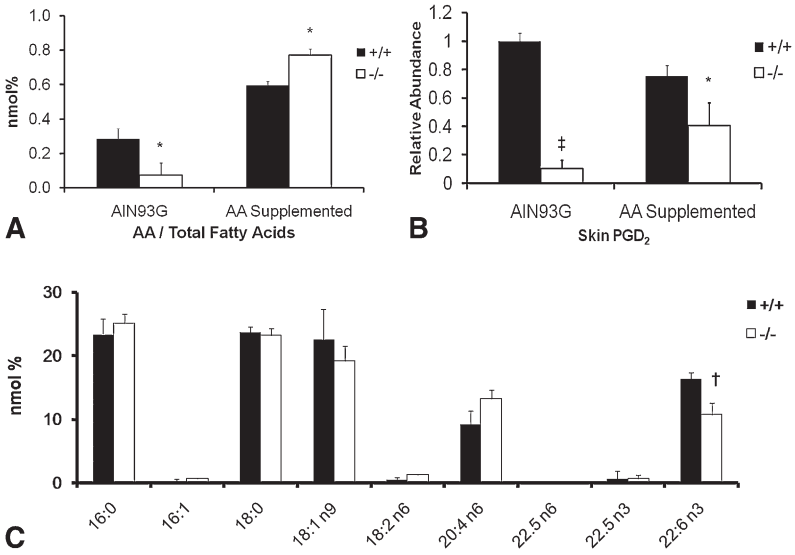

Fig. 8. Effects of dietary supplementation of AA. AIN93G diet with or without 0.4% AA were fed to +/+ and −/− females (n = 3 each). Groups without AA were terminated at 4 months of age, whereas AA supplemented groups were terminated at 8 months of age. A: AA levels in total skin lipid extracts. B: PGD_2 from skin samples. Values are shown relative to the nonsupplemented +/+ group. C: Fatty acid profile of brain total lipid extracts from AA supplemented animals. *$P < 0.05$; †$P < 0.01$; ‡ $P < 0.001$ by Student's *t*-test.

Ulceration of the small intestine was another feature of the −/− mouse. This is also consistent with the human case that showed gastro-intestinal bleeding as a major symptom although ulceration in this mouse model was mild at the time of manifestation of dermatitis. A likely mechanism is a decline of prostaglandin synthesis, similar to the effects seen with NSAIDs. NSAID usage has long been known to produce ulceration in the stomach and small intestine (29). NSAIDs block prostaglandin synthesis by inhibiting cyclooxygenases, leading to an erosion and then ulceration of the mucosal layer. These ulcers are most often seen in the gastric and duodenal region (30), although some studies have shown long-term NSAID users to have ileocecal ulceration as well (31).

HUFAs are highly concentrated in sperm; AA, DPA n-6, and DHA make up 36% of total fatty acids in phospholipids from mouse sperm (32). Also, elongation products of HUFAs are present in sphingolipids (14) and make up to 5% of total fatty acids in sperm (33), implying importance of HUFAs and their products in male fertility. However, a traditional HUFA depletion model was unable to unequivocally demonstrate the essentiality because of accompanying growth retardation and dermatitis. Our −/− model demonstrated the essentiality of HUFAs in spermatogenesis and male fertility. In our model, spermatogenesis was halted just before the spermatids elongate. Considering 99% of HUFAs are localized in the tail of spermatozoa (34), HUFAs are likely indispensable constituents for spermatid elongation.

Although underlying mechanisms of other phenotypes observed in the −/− are yet to be understood, it is possible that part of the phenotypes may be secondary effects of inflammatory lesions such as the dermatitis and intestinal ulcers. For example, this could explain the myeloid hyperplasia observed in the splenic red pulp and the general increase in splenic size and weight in both male and female −/−. In mice, myelopoeis occurs in the spleen, as well as bone marrow, and increases in response to inflammatory conditions. The stress associated with terminal weight loss secondary to trichobezoars may be responsible for the severe thymic lymphoid depletion and impaired follicle maturation observed in the first study (35, 36). However, ovarian changes were also found in subsequent studies in which weight loss did not occur and therefore are a phenotype of the −/−.

While we were preparing this manuscript, Stoffel et al. reported production and characterization of another D6D knockout mouse model (37). Their findings in male and female reproduction are in general agreement with ours; however, there are several notable differences in outcomes. First, we observed that residual HUFAs were present in all tissues examined in −/− animals, whereas Stoffel et al. reported a complete absence of HUFAs in all tissues including testes and liver. This difference cannot be explained by diet, because we used a purified diet that provided adequate LA and ALA but was devoid of HUFAs, whereas they fed a laboratory chow that contained small amounts of HUFAs. Second, all our −/− mice developed severe ulcerative dermatitis around 4 months of age, whereas they did not report dermatitis. The reason of this discrepancy is unknown. However, it should be noted that the manifestation of dermatitis did not require a complete depletion of HUFAs in our study. At the time of dermatitis, nearly half of the DHA remained in testes, and quarter of AA was still present in skin of the −/− mice compared with the +/+. Third, ulceration of the small intestine, similar to that seen with NSAIDs, was another feature of our model, which was not reported by Stoffel et al.

In conclusion, this −/− model has demonstrated the essential need of AA for normal skin function, independent of LA. It has also shown the essentiality of HUFAs in male fertility which could only be inferred previously. The study also showed the absence of D6D isozyme for the first and the last steps of desaturation in DHA and DPA n-6 synthesis. This −/− mouse presents itself as a valuable model to investigate the mechanism of these previously unidentified HUFA functions. Moreover, the model can be used to elucidate DHA function in brain without AA depletion, or DPA n-6 replacement seen in the traditional models. With this model, the investigation into HUFA functions can be greatly advanced.

The authors thank Dr. Jodi Flaws for evaluating ovary histology. ARASCO oil was generously provided by Martek Biosciences Corp., Columbia, MD.

REFERENCES

1. Burr, G. O., and M. M. Burr. 1930. On the nature and role of the fatty acids essential in nutrition. *J. Biol. Chem.* **86:** 587–621.
2. Cho, H. P., M. T. Nakamura, and S. D. Clarke. 1999. Cloning, expression, and nutritional regulation of the mammalian delta-6 desaturase. *J. Biol. Chem.* **274:** 471–477.
3. Williard, D. E., J. O. Nwankwo, T. L. Kaduce, S. D. Harmon, M. Irons, H. W. Moser, G. V. Raymond, and A. A. Spector. 2001. Identification of a fatty acid delta6-desaturase deficiency in human skin fibroblasts. *J. Lipid Res.* **42:** 501–508.
4. Hansen, H. S., and B. Jensen. 1985. Essential function of linoleic acid esterified in acylglucosylceramide and acylceramide in maintaining the epidermal water permeability barrier. Evidence from feeding studies with oleate, linoleate, arachidonate, columbinate and alpha-linolenate. *Biochim. Biophys. Acta.* **834:** 357–363.
5. Hartop, P. J., and C. Prottey. 1976. Changes in transepidermal water loss and the composition of epidermal lecithin after applications of pure fatty acid triglycerides to the skin of essential fatty acid-deficient rats. *Br. J. Dermatol.* **95:** 255–264.
6. Salem, N., Jr., B. Litman, H. Y. Kim, and K. Gawrisch. 2001. Mechanisms of action of docosahexaenoic acid in the nervous system. *Lipids.* **36:** 945–959.
7. Bieri, J. G., and E. L. Prival. 1965. Lipid composition of testes from various species. *Comp. Biochem. Physiol.* **15:** 275–282.
8. Niu, S., D. C. Mitchell, S. Lim, Z. Wen, H. Kim, S. Norman, Jr., and B. J. Litman. 2004. Reduced G protein-coupled signaling efficiency in retinal rod outer segments in response to n-3 fatty acid deficiency. *J. Biol. Chem.* **279:** 31098–31104.
9. Lukiw, W. J., J. G. Cui, V. L. Marcheselli, M. Bodker, A. Botkjaer, K. Gotlinger, C. N. Serhan, and N. G. Bazan. 2005. A role for docosahexaenoic acid-derived neuroprotectin D1 in neural cell survival and Alzheimer disease. *J. Clin. Invest.* **115:** 2774–2783.
10. Mukherjee, P. K., V. L. Marcheselli, C. N. Serhan, and N. G. Bazan. 2004. Neuroprotectin D1: a docosahexaenoic acid-derived docosatriene protects human retinal pigment epithelial cells from oxidative stress. *Proc. Natl. Acad. Sci. USA.* **101:** 8491–8496.
11. Akbar, M., F. Calderon, Z. Wen, and H. Y. Kim. 2005. Docosahexaenoic acid: a positive modulator of Akt signaling in neuronal survival. *Proc. Natl. Acad. Sci. USA.* **102:** 10858–10863.
12. Igarashi, M., J. C. DeMar, Jr., K. Ma, L. Chang, J. M. Bell, and S. I. Rapoport. 2007. Docosahexaenoic acid synthesis from alpha-linolenic acid by rat brain is unaffected by dietary n-3 PUFA deprivation. *J. Lipid Res.* **48:** 1150–1158.
13. Lenzi, A., L. Gandini, V. Maresca, R. Rago, P. Sgro, F. Dondero, and M. Picardo. 2000. Fatty acid composition of spermatozoa and immature germ cells. *Mol. Hum. Reprod.* **6:** 226–231.
14. Sandhoff, R., R. Geyer, R. Jennemann, C. Paret, E. Kiss, T. Yamashita, K. Gorgas, T. P. Sijmonsma, M. Iwamori, C. Finaz, et al. 2005. Novel class of glycosphingolipids involved in male fertility. *J Bio Chem.* **280:** 27310–27318.
15. Nakamura, M. T., A. B. Tang, J. Villanueva, C. H. Halsted, and S. D. Phinney. 1994. Selective reduction of delta 6 and delta 5 desaturase activities but not delta 9 desaturase in micropigs chronically fed ethanol. *J. Clin. Invest.* **93:** 450–454.
16. Cheon, Y., T. Y. Nara, M. R. Band, J. E. Beever, M. A. Wallig, and M. T. Nakamura. 2005. Induction of overlapping genes by fasting and a peroxisome proliferator in pigs: evidence of functional PPARalpha in nonproliferating species. *Am. J. Physiol. Regul. Integr. Comp. Physiol.* **288:** R1525–R1535.
17. Goodman, K. J., and J. T. Brenna. 1992. High sensitivity tracer detection using high-precision gas chromatography-combustion isotope ratio mass spectrometry and highly enriched [U-13C]-labeled precursors. *Anal. Chem.* **64:** 1088–1095.
18. Reeves, P. G., F. H. Nielsen, and G. C. Fahey. 1993. AIN-93 purified diets for laboratory rodents: final report of the American Institute of Nutrition ad hoc writing committee on the reformulation of the AIN-76A rodent diet. *J. Nutr.* **123:** 1939–1951.
19. Moore, K. L., and M. L. Barr. 1954. Nuclear morphology, according to sex, in human tissues. *Acta Anat. (Basel).* **21:** 197–208.
20. Lawrence, P., and J. T. Brenna. 2006. Acetonitrile covalent adduct chemical ionization mass spectrometry for double bond localization in non-methylene-interrupted polyene fatty acid methyl esters. *Anal. Chem.* **78:** 1312–1317.
21. Nakamura, M. T., A. B. Tang, J. Villanueva, C. H. Halsted, and S. D. Phinney. 1992. Reduced tissue arachidonic acid concentration with chronic ethanol feeding in miniature pigs. *Am. J. Clin. Nutr.* **56:** 467–474.
22. Li, Y., T. Y. Nara, and M. T. Nakamura. 2005. Peroxisome proliferator activated receptor-alpha is required for feedback regulation of highly unsaturated fatty acid synthesis. *J. Lipid Res.* **46:** 2432–2440.
23. Sugimoto, M., I. Arai, N. Futaki, Y. Hashimoto, T. Sakurai, Y. Honma, and S. Nakaike. 2006. Time course changes of scratching counts, dermatitis symptoms, and levels of cutaneous prostaglandins in NC/Nga mice. *Exp. Dermatol.* **15:** 875–882.
24. Park, W. J., K. S. D. Kothapalli, P. Lawrence, C. Tyburczy, and J. T. Brenna. 2009. An alternate pathway to long chain polyunsaturates: the FADS2 gene product u8-desaturates 20:2n-6 and 20:3n-3. *J. Lipid Res.* **50:** 1195–1202.
25. Ge, L., J. S. Gordon, C. Hsuan, K. Stenn, and S. M. Prouty. 2003. Identification of the delta-6 desaturase of human sebaceous glands: expression and enzyme activity. *J. Invest. Dermatol.* **120:** 707–714.
26. Miyazaki, M., W. C. Man, and J. M. Ntambi. 2001. Targeted disruption of stearoyl-CoA desaturase1 gene in mice causes atrophy of sebaceous and meibomian glands and depletion of wax esters in the eyelid. *J. Nutr.* **131:** 2260–2268.
27. Matsuda, H., N. Watanabe, G. Geba, J. Sperl, M. Tsudzuki, J. Hiroi, M. Matsumoto, H. Ushio, S. Saito, P. Askenase, et al. 1997. Development of atopic dermatitis-like skin lesion with IgE hyperproduction in NC/Nga mice. *Int. Immunol.* **9:** 461–466.
28. Arai, I., N. Takano, Y. Hashimoto, N. Futaki, M. Sugimoto, N. Takahashi, T. Inoue, and S. Nakaike. 2004. Prostanoid DP1 receptor agonist inhibits the pruritic activity in NC/Nga mice with atopic dermatitis. *Eur. J. Pharmacol.* **505:** 229–235.
29. Bertram, T. A. 2002. Gastrointestinal tract. *In* Handbook of Toxicologic Pathology. W. M. Haschek, C. G. Rousseaux, and M. A. Wallig, editors. Academic Press, San Diego. 121–186.
30. Chiba, T., K. Sato, N. Kudara, H. Shinozaki, K. Ikeda, K. Sato, M. Endo, S. Orii, and K. Suzuki. 2008. Upper gastrointestinal disorders induced by non-steroidal anti-inflammatory drugs. *Inflammopharmacology.* **16:** 16–20.
31. Kurahara, K., T. Matsumoto, M. Iida, K. Honda, T. Yao, and M. Fujishima. 2001. Clinical and endoscopic features of nonsteroidal anti-inflammatory drug-induced colonic ulcerations. *Am. J. Gastroenterol.* **96:** 473–480.
32. Rejraji, H., B. Sion, G. Prensier, M. Carreras, C. Motta, J. M. Frenoux, E. Vericel, G. Grizard, P. Vernet, and J. R. Drevet. 2006. Lipid remodeling of murine epididymosomes and spermatozoa during epididymal maturation. *Biol. Reprod.* **74:** 1104–1113.
33. Poulos, A., P. Sharp, D. Johnson, I. White, and A. Fellenberg. 1986. The occurrence of polyenoic fatty acids with greater than 22 carbon atoms in mammalian spermatozoa. *Biochem. J.* **240:** 891–895.
34. Connor, W. E., D. S. Lin, D. P. Wolf, and M. Alexander. 1998. Uneven distribution of desmosterol and docosahexaenoic acid in the heads and tails of monkey sperm. *J. Lipid Res.* **39:** 1404–1411.
35. Kuper, C. F., E. de Heer, H. Van Loveren, and J. G. Voss. 2002. Immune system. *In* Handbook of Toxicologic Pathology. W. M. Haschek, C. G. Rousseaux, and M. A. Wallig, editors. Academic Press, San Diego. 585–646.
36. Yuan, Y., and G. L. Foley. 2002. Female reproductive system. *In* Handbook of Toxicologic Pathology. W. M. Haschek, C. G. Rousseaux, and M. A. Wallig, editors. Academic Press, San Diego. 847–894.
37. Stoffel, W., B. Holz, B. Jenke, E. Binczek, R. H. Gunter, C. Kiss, I. Karakesisoglou, M. Thevis, A. A. Weber, S. Arnhold, et al. 2008. Delta6-Desaturase (FADS2) deficiency unveils the role of omega3- and omega6-polyunsaturated fatty acids. *EMBO J.* **27:** 2281–2292.